J Biomol NMR (2015) 62:53–61
DOI 10.1007/s10858-015-9916-9

ARTICLE

# Simultaneous acquisition of 2D and 3D solid-state NMR experiments for sequential assignment of oriented membrane protein samples

**T. Gopinath[1] · Kaustubh R. Mote[2] · Gianluigi Veglia[1,2]**

Received: 13 January 2015 / Accepted: 3 March 2015 / Published online: 7 March 2015


**Abstract** We present a new method called DAISY (Dual Acquisition orIented ssNMR spectroScopY) for the simultaneous acquisition of 2D and 3D oriented solid-state NMR experiments for membrane proteins reconstituted in mechanically or magnetically aligned lipid bilayers. DAISY utilizes dual acquisition of sine and cosine dipolar or chemical shift coherences and long living $^{15}$N longitudinal polarization to obtain two multi-dimensional spectra, simultaneously. In these new experiments, the first acquisition gives the polarization inversion spin exchange at the magic angle (PISEMA) or heteronuclear correlation (HETCOR) spectra, the second acquisition gives PISEMA-mixing or HETCOR-mixing spectra, where the mixing element enables inter-residue correlations through $^{15}$N–$^{15}$N homonuclear polarization transfer. The analysis of the two 2D spectra (first and second acquisitions) enables one to distinguish $^{15}$N–$^{15}$N inter-residue correlations for sequential assignment of membrane proteins. DAISY can be implemented in 3D experiments that include the polarization inversion spin exchange at magic angle via I spin coherence (PISEMAI) sequence, as we show for the simultaneous acquisition of 3D PISEMAI–HETCOR and 3D PISEMAI–HETCOR-mixing experiments.

This paper is dedicated to John Waugh for inspiring our research with his pioneering work on the separated local fields experiments.

✉ Gianluigi Veglia
vegli001@umn.edu

[1] Department of Biochemistry, Molecular Biology, and Biophysics, University of Minnesota, 6-155 Jackson Hall, 321 Church St. SE, Minneapolis, MN 55455, USA

[2] Department of Chemistry, University of Minnesota, Minneapolis, MN 55455, USA

**Keywords** Simultaneous acquisition · Oriented solid-state NMR · Membrane proteins · Bicelles · Aligned lipid bilayers

## Introduction

The folding and function of membrane proteins are shaped by lipid membranes (Phillips et al. 2009). Therefore, a complete understanding of their structure–function relationships is possible only by characterizing the structures and dynamics of these proteins in native-like lipid bilayer environments. To this extent, oriented sample solid-state NMR (OS ssNMR) represents a powerful technique that enables the measurement of anisotropic NMR parameters for membrane proteins embedded in lipid membranes in the liquid crystalline phase (Veglia et al. 2012). Unlike the more popular magic angle spinning (MAS) technique, OS ssNMR necessitates the careful preparation of membrane protein samples in magnetically or mechanically aligned lipid membranes (Das et al. 2013). Although labor intensive, these preparations make it possible to more accurately control the parameters that contribute to the formation of well-oriented samples, such as hydration, lipid composition and phase, as well as membrane architecture. A key experiment for measuring anisotropic NMR parameters for aligned membrane proteins is the separated local fields (SLF) experiment developed by John Waugh (Waugh 1976). SLF experiments enable one to separate anisotropic NMR parameters such as $^{15}$N chemical shift (CS) and $^{15}$N–$^{1}$H dipolar coupling (DC) in two dimensions. The most common versions of SLF experiments are PISEMA ( Wu et al. 1994, 1995), SAMPI4 (Nevzorov et al. 2007), and HIMSELF (Dvinskikh et al. 2006), which are routinely used to analyze the topology of membrane bound proteins and peptides (Miao and Cross 2013; Murray et al. 2013). In addition,

HETCOR experiments are also used to measure $^{1}H$ and $^{15}N$ anisotropic chemical shifts (Marassi et al. 2000), offering additional restraints to define the structure and architecture of membrane proteins (Fu et al. 2007). Historically, these experiments have suffered from poor sensitivity and resolution. In recent years, we significantly improved the performance of these experiments by implementing a sensitivity-enhanced (SE) element that enabled us to acquire both 2D and 3D spectra of membrane proteins aligned in lipid bicelles or bilayers (Gopinath et al. 2013). However, resonance assignment remains the Achilles' hill of OS ssNMR. Although SLF and HETCOR spectra of U–$^{15}N$ labeled proteins give rise to regular patterns that are used to fingerprint membrane protein backbone topology (Marassi and Opella 2000; Mascioni et al. 2004; Mascioni and Veglia 2003; Mesleh et al. 2002; Wang et al. 2000), atomic-resolution structure determination requires residue-specific assignments of the ssNMR spectra (Mote et al. 2013; Traaseth et al. 2009; Verardi et al. 2011; Vostrikov et al. 2013). For single-pass membrane proteins, the regular patterns of the SLF spectra together with selective labeling of amino acids are often sufficient to assign the backbone resonances. However, this approach fails when deviations from ideal helices occur or when multispan membrane proteins are analyzed. In these cases, the amide resonance chemical shifts and dipolar coupling correlations can be severely overlapped. A possible strategy to obtain backbone sequential assignments is to combine SLF experiments with through-space correlations of backbone amide nitrogens via $^{15}N$–$^{15}N$ polarization transfer schemes (Knox et al. 2010; Tang et al. 2012). There are three different strategies to accomplish polarization transfer: homonuclear $^{15}N$–$^{15}N$ polarization transfer via proton-driven spin diffusion (PDSD) (Suter and Enrnst 1985; Szeverenyi et al. 1982), cross-relaxation driven spin diffusion (CRDSD) (Xu et al. 2008), or mismatch Hartmann–Hahn (MMHH) (Nevzorov 2008). While PDSD uses longitudinal polarization transfer and provides sequential $^{15}N$–$^{15}N$ correlations, CRDSD and MMHH are both based on transverse polarization transfer and provide long-range inter-residue correlations (up to 10 Å). A systematic study of these three polarization transfer techniques has been reported by our group, where we noted that the relative sensitivity of these experiments plays an important role in the design of the experiment to be carried out (Traaseth et al. 2010). In fact, high lipid-to-protein ratios are often necessary to obtain well-ordered bicellar phases (Veglia et al. 2012). As a result, ordered bicelle preparations contain only a few milligrams of U–$^{15}N$ labeled proteins, making their spectroscopic analysis quite challenging. In addition, the current probe technology, although significantly improved with the low-E coils (Gor'kov et al. 2007), requires long relaxation delays to prevent sample overheating. For these reasons, we propose a new method called DAISY (Dual Acquisition orIented ssNMR spectroScopY) that enables the acquisition of two OS ssNMR spectra, simultaneously. The overall philosophy of this approach impinges on our recent developments in the field of MAS NMR sequences for the dual and multiple acquisitions of 2D and 3D experiments (Gopinath and Veglia 2012a, b, 2013). Specifically, we make use of the long living $^{15}N$ polarization to acquire two experiments with only one pulse sequence and without the addition of a second receiver.

We demonstrate the performance of DAISY for the simultaneous acquisition of 2D PISEMA and 2D PISEMA-mixing experiments as well as 2D HETCOR and 2D HETCOR-mixing experiments. Finally, we also implemented a 3D experiment to simultaneously acquire PISEMAI–HETCOR and PISEMAI–HETCOR-mixing spectra. DAISY can be used with other variants of SLF, HETCOR and homonuclear mixing sequences and will speed up the acquisition of OS experiments without additional hardware.

## Materials and methods

### Sample preparation

U–$^{15}N$ labeled sarcolipin (SLN) was expressed in *E. coli* bacteria and purified as reported previously (Buck et al. 2003). Bicelles were prepared by drying 37.2 mg of DMPC and 7.6 mg of DHPC in chloroform into separate glass vials under a stream of $N_2$ gas (DMPC/DHPC molar ratio of 3.2/1). Approximately 2 mg of SLN were reconstituted in a DHPC micelle solution, which was then added to DMPC lipids. Bicelles were formed after 3–5 freeze/thaw cycles, which resulted in a non-viscous solution between 0 and 15 °C and a viscous and clear solution above 30 °C. To align the bicelles with the bilayer normal parallel to the static magnetic fields, we doped our preparations with 5 mM $YbCl_3$. The final volume was adjusted to 160 µL by addition of NMR buffer, giving a final lipid concentration of 28 % (w/v). The NAL crystal was prepared as reported by Carroll et al. (1990).

### NMR experiments

All of the NMR experiments were performed on an Agilent VNMRS spectrometer operating at a $^{1}H$ frequency of 700 MHz and equipped with a low-E bicelle probe built by the RF program at the National High Magnetic Field Laboratory (NHMFL) in Florida (Gor'kov et al. 2007). A cross-polarization (CP) time of 1 ms was applied with $^{1}H$ and $^{15}N$ RF amplitudes set to 50 kHz. 5 µs 90° pulses were used for $^{1}H$ and $^{15}N$, and a 50 kHz SPINAL decoupling (Manning et al. 2002) was used on $^{1}H$ during the $^{15}N$ acquisition period. A recycle delay of 3 s and an acquisition time of 15 ms were used with identical parameters for both acquisition periods ($t_2'$ and $t_2''$ or $t_2'$ and $t_3''$). All the spectra

were acquired with a $\tau_1$ value set to 1 ms to dephase any residual transverse magnetization. For SLN, the $^{15}N$–$^{15}N$ transfer was obtained using a 3 s PDSD mixing time ($\tau_{mix}$), whereas for the NAL single crystal a 6 ms MMHH mixing time was used. For the PISEMA experiments, the FSLG sequence was used on the $^1H$ channel during the $t_1$ period with an effective RF amplitude of 62.5 kHz. A phase-switched spin-lock was applied on the $^{15}N$ channel with a 62.5 kHz RF amplitude. The $\tau$ delay was set to 100 μs with an FSLG effective field corresponding to 80 kHz. For the HETCOR experiments, the FSLG homonuclear decoupling was used during $t_1$ with $^1H$ and $^{15}N$ RF amplitudes of 62.5 and 30 kHz, respectively. During the WIM24 heteronuclear polarization transfer, 90° pulses of 5 μs duration were used on both $^1H$ and $^{15}N$ with a $\tau$ delay set to 192 μs. The 2D spectra of the NAL crystal were acquired with 16 scans and 64 increments for 2D PISEMA and 32 increments for 2D HETCOR experiments. The 3D PISEMAI–HETCOR experiment was acquired with 8 scans with 16 $t_1$ and $t_2$ increments. Note that in the PISEMAI block the polarization inversion spin exchange at magic angle occurs via I spin dipolar coherence, dramatically increasing the signal (Gopinath et al. 2010a). For SLN, a total of 5000 scans and 20 $t_1$ increments were used for simultaneous acquisition of the 2D PISEMA and 2D PISEMA-mixing experiments.

from homonuclear DC interactions by means of homonuclear dipolar decoupling pulse scheme during $t_1$. The *S* spins will then evolve under the CS Hamiltonian during the $t_2$ acquisition period, resulting in a two-dimensional spectrum that correlates the *S* spin chemical shift with *I*–*S* DC. In the SE version, a spin-echo is utilized to recover both sine and cosine modulated dipolar coherences, thereby enhancing the signal up to 40 % (Gopinath et al. 2010a, b, 2013; Gopinath and Veglia 2009). In the new experiment reported in Fig. 1a, we utilize the dual acquisition method to separate sine and cosine coherences and give two separate spectra: 2D PISEMA and PISEMA-mixing. In this pulse scheme (Fig. 1a), the polarization is transferred from $^1H$ to $^{15}N$ (I to S) via Hartmann–Hahn CP, a 35° pulse on $^1H$ creates the polarization inversion state ($I_z$-$S_z$) in the doubly tilted rotating frame. During the $t_1$ period, the $I_z$-$S_z$ term evolves under zero quantum dipolar Hamiltonian, thereby creating cosine and sine dipolar coherences. After $t_1$ evolution, a 90° pulse is applied to store the cosine dipolar coherence along the z-direction, whereas the two-spin order sine dipolar coherence is converted into a single spin term in the following $2\tau$ period and detected during the first acquisition period to give a PISEMA spectrum. The evolution of the polarization is summarized as follows:

$$
\begin{aligned}
&I_z \xrightarrow{90^\circ_y} I_x \xrightarrow{CP} -I_x + S_x \\
&\xrightarrow{35^\circ_y - U'} -I_z + S_z \xrightarrow{H'(t_1)-(U')^{-1}} S_x \cos(S_{PISEMA}\omega_{IS}t_1) + 2I'_zS_y \sin(S_{PISEMA}\omega_{IS}t_1) \\
&\xrightarrow{(90)^{I,S}_{-y} - H''(2\tau)} S_z \cos(S_{PISEMA}\omega_{IS}t_1) + S_x \cdot \sin(S_{FSLG}\omega_{IS}\tau) \cdot \sin(S_{PISEMA}\omega_{IS}t_1) \\
&\xrightarrow{H'(t'_2)} S_z \cos(S_{PISEMA}\omega_{IS}t_1) + \left[S_x \cdot \sin(S_{FSLG}\omega_{IS}\tau) \cdot \sin(S_{PISEMA}\omega_{IS}t_1) \cdot e^{i\omega_s t'_2}\right]_{1st-acquisition} \\
&\text{where } U' = e^{-i\theta_m I_y} \cdot e^{-i(\pi/2)S_y},\ H'(t_1) = S_{PISEMA} \cdot \omega_{IS} \cdot \left(2I_xS_x + 2I_yS_y\right), \\
&\quad U'' = e^{-i\theta_m I_y},\ H''(2\tau) = S_{FSLG} \cdot \omega_{IS} \cdot 2I_zS_z, \text{ and } \omega_{IS} = 2\pi \cdot D_{IS}
\end{aligned}
\tag{1}
$$

## Results

### Simultaneous acquisition of PISEMA and PISEMA-mixing experiments

In a typical rotating frame SLF experiment (Ramamoorthy and Yamamoto 2006), polarization is transferred from the abundant *I* spin ($^1H$) bath to the *S* spins ($^{15}N$ or $^{13}C$) to generate $S_x$ polarization that evolves for a $t_1$ period under *I*–*S* DC. The heteronuclear DC Hamiltonian is isolated

In Eq. 1, $U'$ and $U''$ refer to the rotating frame transformations and $\theta_m$ is the magic angle; $S_{PISEMA}$, and $S_{FSLG}$ are dipolar scaling factors during $t_1$ and $\tau$ periods, respectively; $D_{IS}$ and $\omega_s$ are the *I*–*S* DC and S spin CS. The cosine dipolar term evolves through the mixing period followed by the second acquisition, giving a 2D PISEMA-mixing spectrum. Depending on the proximity of the $^{15}N$ spin pairs as well as the length and type of mixing sequence (Fig. 1b), each $S_z$ spin operator creates multiple cross peak terms ($\sum_i S_x^i$) resulting from $^{15}N$–$^{15}N$ polarization transfer:

$$
\begin{aligned}
S_z\cos(S_{PISEMA}\omega_{IS}t_1) &\xrightarrow{mixing}\left(S_x+\sum_i S_x^i\right)\cdot\cos(S_{PISEMA}\omega_{IS}t_1)\\
&\xrightarrow{t_2''}\left[\left(S_x+\sum_i S_x^i\right)\cdot\cos(S_{PISEMA}\omega_{IS}t_1)\right.\\
&\quad\left.\cdot e^{i\omega_s t_2}\right]_{2nd-acquisition}
\end{aligned}
\tag{2}
$$

where $S_x^i = e^{-iH\tau_{\mathrm{mix}}}\cdot S_x\cdot e^{iH\tau_{\mathrm{mix}}}$. In the latter expression, H is the rotating frame Hamiltonian for PDSD, MMHH, or CRDSD (Traaseth et al. 2010) and $\tau_{\mathrm{mix}}$ is the length of the mixing period. Note that the $^{15}$N nuclei have long $T_1$ relaxation times, hence the cosine dipolar term can be stored without loss of polarization while recording the first FID. For the PDSD sequence, a 90° pulse is applied after the longitudinal mixing, while for the MMHH and CRDSD sequences the 90° pulse is applied prior to transverse mixing. The mixing times (τ) are typically 3 s, 10 ms, and 6 ms for PDSD, CRDSD, and MMHH, respectively. As we have shown previously, the PDSD sequence gives optimal cross peak intensities for sequential (i, i+1) correlations; on the other hand, the CRDSD and MMHH are more efficient for long-range distances of 6–10 Å.

To demonstrate the performance of DAISY, we used the pulse sequence in Fig. 1a to acquire 2D PISEMA and PISEMA-mixing experiments both on a single crystal of N-acetyl-leucine (NAL) and SLN in oriented bicelles. Figure 2a shows PISEMA and PISEMA-mixing experiments on the NAL crystal using the MMHH polarization transfer scheme with a 6 ms mixing period. The four fold symmetry of the crystal unit generates a set of four distinct resonances with different values of the CS and DC. For SLN, we obtained intense cross peaks between sequential residues using a 3 s PDSD transfer (Fig. 3). The sequential (i,i+1) inter-residue cross peak positions are in close agreement with the previous resonance assignments for this protein obtained from a 3D version of PDSD experiment.

## Simultaneous acquisition of 2D HETCOR and HETCOR-mixing experiments

The heteronuclear correlation (HETCOR) experiment maps $^1$H and $^{15}$N chemical shifts of $^{15}$N–$^1$H spin systems. Sequential assignment can also be achieved via proton dimension by incorporating $^{15}$N–$^{15}$N mixing in a 2D HETCOR experiment. For this purpose, we designed a new pulse scheme to simultaneously acquire two 2D experiments, HETCOR and HETCOR-mixing as reported in Fig. 1c. A 90° pulse creates $^1$H single quantum coherence followed by chemical shift evolution during $t_1$ under FSLG homonuclear decoupling (Bielecki et al. 1990). $^{15}$N spins are decoupled during $t_1$ evolution using continuous wave (CW) decoupling. Cosine and sine modulated $^1$H chemical shift spin operators ($I_x$ and $I_z$) are then transferred to $^{15}$N using WIM24 (Windowless Isotropic Mixing) cross polarization (Caravatti et al. 1983). The transverse polarization ($I_x$) is acquired during the first acquisition ($t_2'$), whereas the longitudinal polarization undergoes homonuclear $^{15}$N–$^{15}$N longitudinal/transverse mixing followed by the second acquisition ($t_2''$). The phase ϕ of the 90° pulse prior to WIM transfer is alternated between x and y for the States mode of acquisition in the $t_1$ dimension. A two-dimensional Fourier transform of the first ($t_1$, $t_2'$) and second ($t_1$, $t_2''$) acquisitions gives the 2D HETCOR and HETCOR-mixing spectra, respectively, where the cross peaks associated with each $^{15}$N–$^1$H spin system are displayed along the $^{15}$N dimension. The evolution of the polarization is described as it follows:

$$
\begin{aligned}
&I_z \xrightarrow{(90_x^\circ)^I} -I_y\\
&\xrightarrow{H_{FSLG}(t_1)} -I_y\cos(S_{FSLG}\omega_{IS}t_1) - I_x'\sin(S_{FSLG}\omega_{IS}t_1)\\
&\xrightarrow{\left(54_y^\circ\right)^{\mathrm{I}}-\left(90_{\phi-x\,\mathrm{ory}}^\circ\right)^I} -I_y e^{iS_{FSLG}\omega_I t_1} - I_z e^{iS_{FSLG}\omega_I t_1}\\
&\xrightarrow{H_{WIM24}(\tau_1)} -\frac{1}{2}[1-\cos(S_{WIM24}\omega_{IS}\tau_1)]\cdot\left[S_y e^{iS_{FSLG}\omega_I t_1} + S_z e^{iS_{FSLG}\omega_I t_1}\right]\\
&\xrightarrow{t_2'-mixing-t_2''} -\frac{1}{2}[1-\cos(S_{WIM24}\omega_{IS}\tau_1)]\cdot\left\{\begin{array}{l}\left[S_y\cdot e^{iS_{FSLG}\omega_I t_1}\cdot e^{i\omega_S t_2'}\right]_{1st-acquisition}\\ +\left[\left(S_y+\sum_i S_y^i\right)\cdot e^{iS_{FSLG}\omega_I t_1}\cdot e^{i\omega_S t_2'}\right]_{2nd-acquisition}\end{array}\right\}
\end{aligned}
\tag{3}
$$

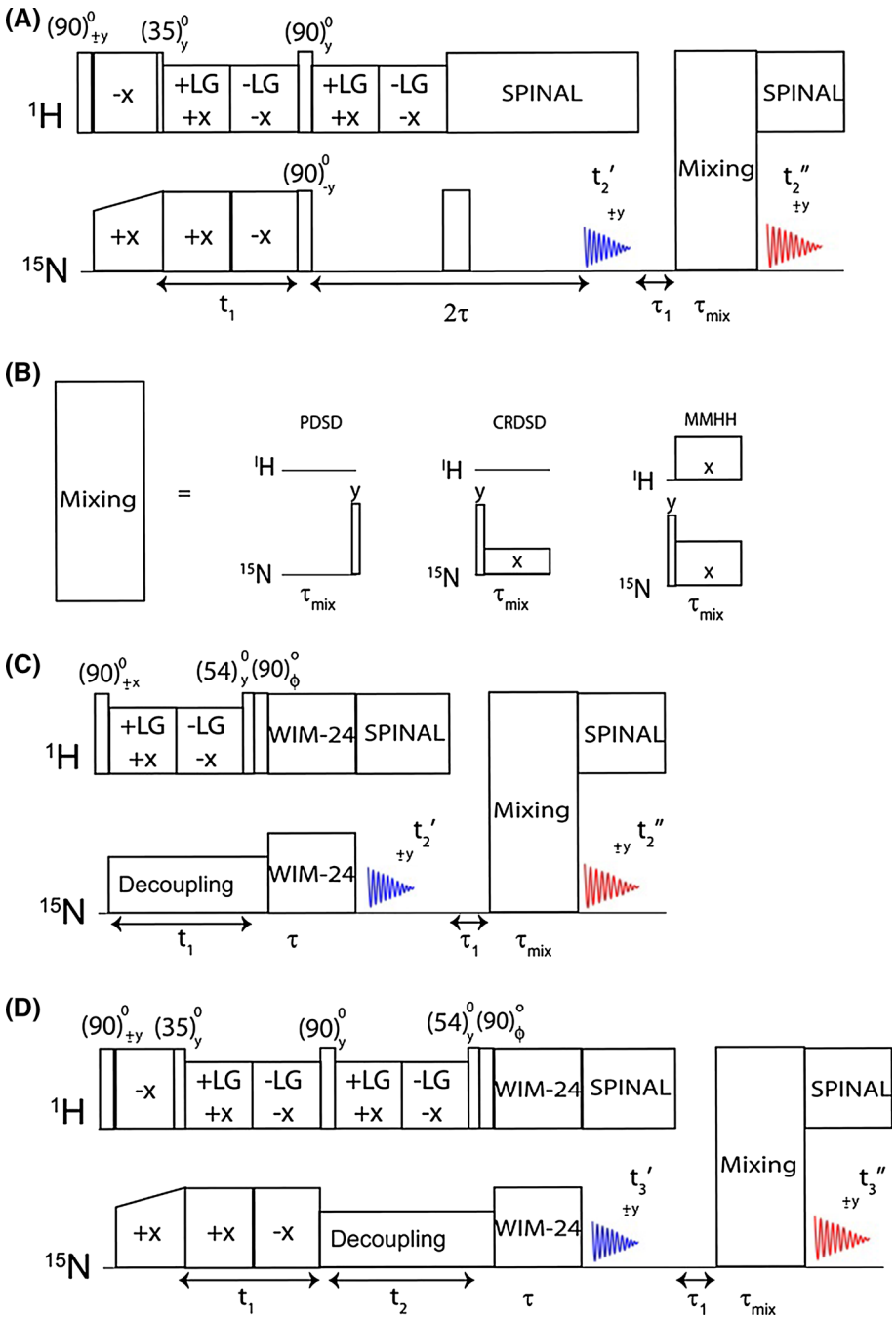


**Fig. 1** **a** Pulse sequence for simultaneous acquisition of PISEMA and PISEMA-mixing experiments corresponding to the first and second acquisitions, respectively. One of the mixing sequences shown in **b** is used prior to the second acquisition. **c** Pulse sequence for the simultaneous acquisition of HETCOR and HETCOR-mixing experiments. **d** Pulse sequence for the simultaneous acquisition of two 3D experiments (PISEMAI–HETCOR and PISEMAI–HETCOR-mixing experiments)

In Eq. 3, $\omega_I$ and $\omega_s$ are the chemical shifts for spin I and S, respectively, and $S_{WIM24}$ is the scaling factor ($\sim$0.66) for the WIM24 sequence. $\sum_i S_x^i$ indicates the cross peaks as for Eq. 2. Figure 2b shows the HETCOR and HETCOR-mixing spectra of NAL single crystal using the pulse sequence of Fig. 1b, with a 6 ms MMHH mixing period prior to the second acquisition.

## Simultaneous acquisition of 3D experiments

The pulse sequence of Fig. 1b can be easily extended to a 3D experiment by incorporating $^{15}$N–$^{1}$H DC evolution prior to the $^{1}$H CS evolution period. This modification results in the pulse sequence reported in Fig. 1d, which enables the acquisition of 3D PISEMAI–HETCOR and

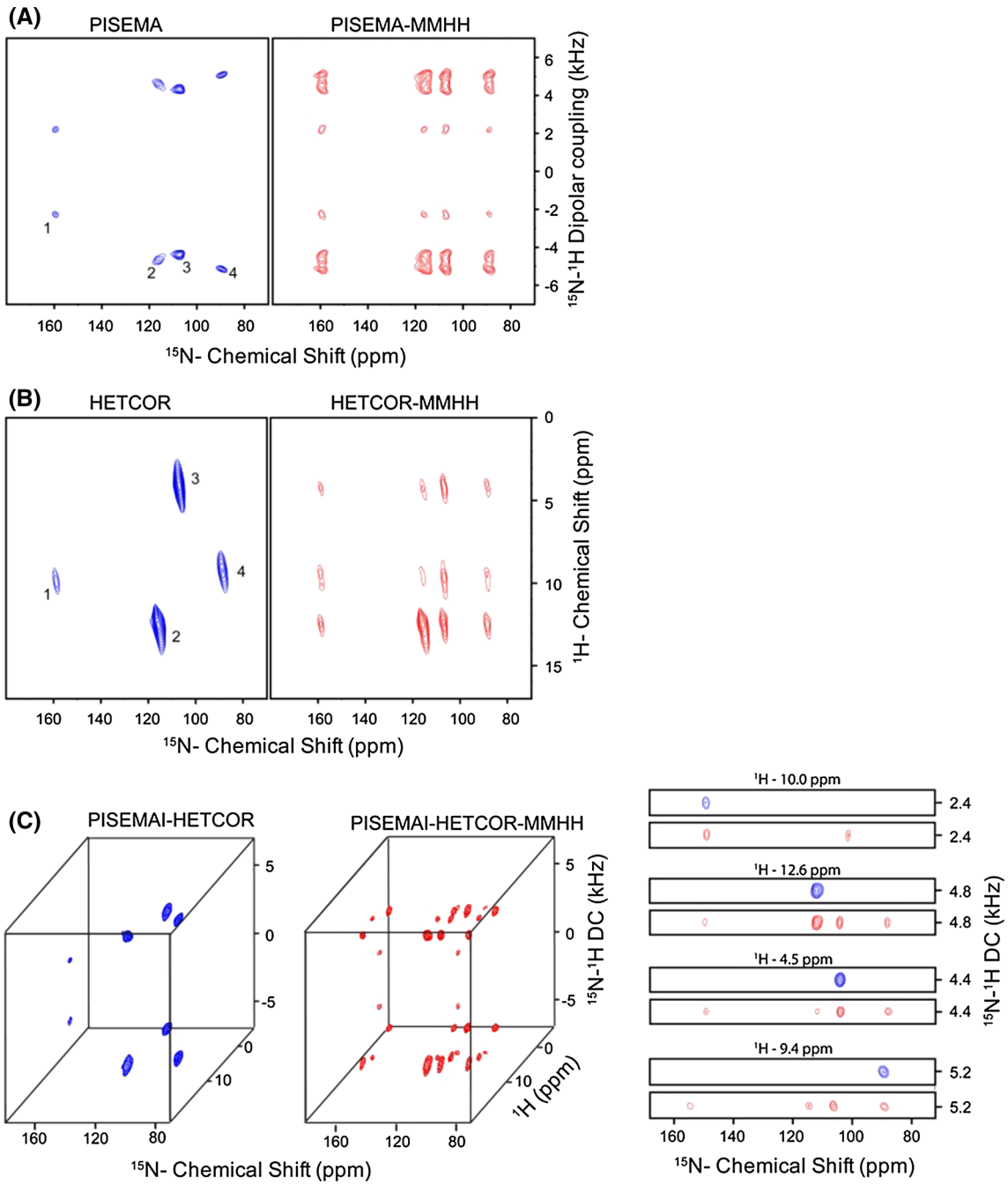


**Fig. 2** Simultaneous acquisition of two and three-dimensional experiments on a NAL single crystal using the pulse sequences shown in Fig. 1. **a** PISEMA and PISEMA-mixing, **b** HETCOR and HETCOR-mixing, **c** 3D PISEMAI-HETCOR and PISEMAI–HETCOR-mixing spectra obtained from pulse sequences shown in Fig. 1. MMHH (Fig. 1**b**) was used with a 6 ms mixing period prior to the second acquisition. The spectra obtained in the first and second acquisitions (Fig. 1) are shown in *blue* and *red colors* respectively. The cross peaks resulting from $^{15}$N–$^{15}$N mixing can be identified in the *red* spectra (along $^{15}$N dimension). Peaks from *left* to *right* in the $^{15}$N dimension are labeled as 1, 2, 3, and 4. The 2D *strip plots* shown in **c** are taken along the $^{1}$H chemical shift dimension of the 3D spectra

PISEMAI–HETCOR-mixing experiments in the first and second acquisitions, respectively. The spin operator formalism is similar to Eqs. 1–3, where the $^{1}$H dipolar coherences are evolved during the $t_1$ evolution period, and the chemical shift evolution takes place during $t_2$, which is followed by WIM24 CP. As for the HETCOR experiment, two polarization transfer pathways result from the WIM24-CP sequence, which are then used to record 3D PISEMAI–HETCOR and PISEMAI–HETCOR-mixing experiments. To test this pulse sequence, we used an NAL single crystal;

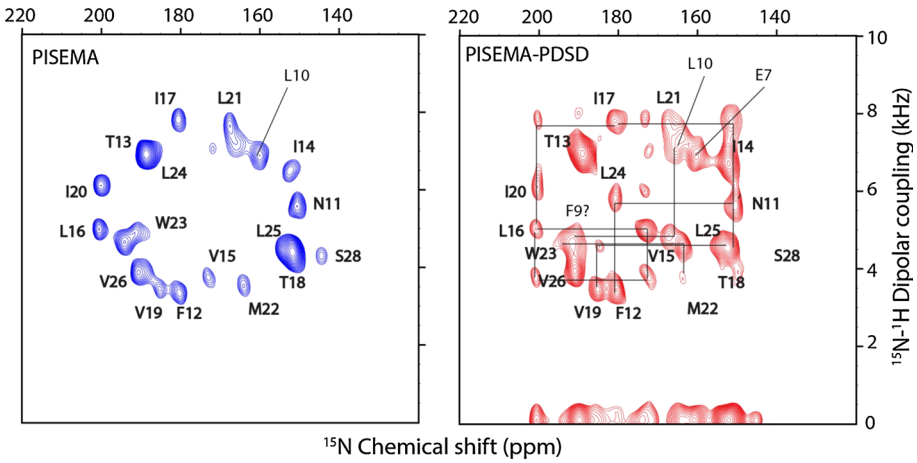


**Fig. 3** PISEMA and PISEMA–PDSD spectra of sarcolipin (SLN), acquired simultaneously using the pulse sequence shown in Fig. 1**a**. PDSD mixing time of 3 s was used prior to the second acquisition. The cross peaks in the PISEMA–PDSD spectrum are identified by comparing with the reference PISEMA spectrum shown in *blue*. The cross peak positions are in agreement with previous assignment taken from reference (Mote et al. 2011)

the resulting 3D PISEMAI-HETCOR and 3D PISEMAI–HETCOR-mixing spectra are shown in Fig. 2c.

## Discussion

Oriented solid-state NMR is the most direct method to obtain the tilt and azimuthal angles of membrane proteins and peptides with respect to the lipid bilayer (Aisenbrey et al. 2013; Marassi and Opella 2000; Wang et al. 2000). A significant advantage of this approach is that the orientational restraints can be derived from the analytical expression of DC and CS values, or alternatively, obtained by refining protein structures using these values as harmonic restraints in simulated annealing calculations (De Simone et al. 2014; Shi et al. 2009). While the assignment procedures of microcrystalline and membrane proteins under magic angle spinning (MAS) conditions are now established (Hong et al. 2012; McDermott 2009; Siegal et al. 1999; Wang and Ladizhansky 2014), assignment continues to be a major bottleneck for OS ssNMR (Veglia et al. 2012) and in many cases site-specific resonance assignment can only be obtained using selectively labeled peptides and proteins (Michalek et al. 2013; Resende et al. 2014). A first example of the sequential assignment of a membrane protein was demonstrated for M2 domain of the influenza virus by Opella and co-workers (Marassi et al. 2000). Also, Nevzorov and co-workers proposed a 2D SLF experiment in which a $^{15}$N–$^{15}$N MMHH scheme was used during the mixing period after DC evolution to sequentially assign the fd coat protein, with the assignment of the cross peaks of the SLF spectrum by comparison with the classical SLF spectrum (Knox et al. 2010; Tang et al. 2012). Our group recently applied a similar approach for the sequential resonance assignments of SLN in lipid bicelles using both 2D and 3D oriented solid-state NMR experiments (Mote et al. 2013). The new method DAISY presented here takes one step forward in the assignment protocol of oriented membrane proteins by integrating PISEMA and HETCOR experiments with $^{15}$N–$^{15}$N polarization transfer. Sequential assignment of $^{15}$N–$^{1}$H spin pairs can be obtained by comparing two spectra acquired simultaneously, thus avoiding the discrepancies in resonance positions due to different sample preparations and/or spectrometer instability. For single pass membrane proteins, the 2D version of DAISY shown in Fig. 1a, b can used as a quick method for confirming the topology together with other experimental data and/or along with pattern recognition such as PISA wheels (Marassi and Opella 2000; Mascioni et al. 2004; Mascioni and Veglia 2003; Mesleh et al. 2002; Wang et al. 2000). As shown in Fig. 2 for a NAL single crystal in arbitrary orientation, peaks 1 and 4 are well resolved in the dipolar dimension (Fig. 2a), whereas peaks 2 and 3 are resolved in the $^{1}$H dimension (Fig. 2b). This leads to ambiguous cross peak intensities for overlapped resonances in the F1 dimension of the 2D spectra. On the other hand, the 3D spectra shown in Fig. 2c resolves all four peaks in either the $F_1$ (DC) or $F_2$ ($^{1}$H CS) indirect dimensions.

Figure 3 shows the application of DAISY to SLN reconstituted in oriented in lipid bicelles. While the spectra of the single-span membrane protein SLN are relatively well-resolved, multispan membrane proteins display fairly overlapped spectra; in these cases, the 3D experiments will be crucial to determine the assignments of the spectra. A shortcoming of this approach is the low sensitivity of the second FID. This is due to weak polarization transfer efficiency among $^{15}$N nuclei as well as $T_1$ or $T_{1\rho}$ relaxation effects during the $^{15}$N–$^{15}$N mixing period. In other words, the first acquisition does not require as many scans as the second acquisition. However, the first acquisition that gives a reference spectrum may be counted a bonus if one decides to acquire 2D or 3D sequential correlation experiments. Moreover, the simultaneous acquisition of

reference and the cross peaks spectra avoids the possibility of misinterpreting the peak positions caused by sample or spectrometer instability. Although this method is demonstrated for membrane proteins embedded in bicelle preparations, it can also be applied to mechanically aligned membrane proteins. Of course, broader lines of mechanically aligned samples will limit cross peak resolution, as bicelles give rise to sharper $^{15}$N resonances (Durr et al. 2012) However, based on the improvements in sample preparation, spectroscopy, and probe technology, we believe that DAISY represents a promising avenue by which to expand the boundaries of OS ssNMR.

## Conclusions

Although selective labeling and computational approaches will continue to be important, sequential assignment is the only approach that allows full assignment of large membrane proteins. The new method presented in this paper (DAISY) enables one to acquire two PISEMA spectra simultaneously, with and without $^{15}$N–$^{15}$N homonuclear polarization transfer. These two spectra together can be used for the sequential assignment of the $^{15}$N–$^{1}$H spin systems of membrane proteins. Furthermore, DAISY was implemented for 2D HETCOR as well as 3D PISEMAI–HETCOR experiments. Together with recent developments in sample preparations and probe technology, the application of sensitivity enhanced methods (Gopinath et al. 2013) and dual acquisition methods such as DAISY will lead to the high-throughput determination of the structural topology of membrane proteins.

**Acknowledgments** This work is supported by the National Institute of Health (GM 64742 and GM 72701). The NMR experiments were carried out at the Minnesota NMR Center.

## References

Aisenbrey C, Michalek M, Salnikov ES, Bechinger B (2013) Solid-state NMR approaches to study protein structure and protein–lipid interactions. Methods Mol Biol 974:357–387. doi:10.1007/978-1-62703-275-9_16

Bielecki A, Kolbert AC, de Groot HJM, Griffin RG, Levitt MH (1990) Frequency-switched Lee-Goldburg sequences in solids. Adv Magn Reson 14:111–124

Buck B, Zamoon J, Kirby TL, DeSilva TM, Karim C, Thomas D, Veglia G (2003) Overexpression, purification, and characterization of recombinant Ca-ATPase regulators for high-resolution solution and solid-state NMR studies. Protein Expr Purif 30:253–261

Caravatti P, Braunschweiler L, Ernst RR (1983) Heteronuclear correlation spectroscopy in rotating solids. Chem Phys Lett 100:305–310. doi:10.1016/0009-2614(83)80276-0

Carroll PJ, Stewart PL, Opella SJ (1990) Structures of two model peptides: N-Acetyl-D, L-Valine and N-Acetyl-L-Valyl-L-Leucine. Acta Crystallogr, Sect C 46:243–246

Das N, Murray DT, Cross TA (2013) Lipid bilayer preparations of membrane proteins for oriented and magic-angle spinning solid-state NMR samples. Nat Protoc 8:2256–2270. doi:10.1038/nprot.2013.129

De Simone A, Mote KR, Veglia G (2014) Structural dynamics and conformational equilibria of SERCA regulatory proteins in membranes by solid-state NMR restrained simulations. Biophys J 106:2566–2576. doi:10.1016/j.bpj.2014.03.026

Durr UH, Gildenberg M, Ramamoorthy A (2012) The magic of bicelles lights up membrane protein structure. Chem Rev 112:6054–6074. doi:10.1021/cr300061w

Dvinskikh SV, Yamamoto K, Ramamoorthy A (2006) Heteronuclear isotropic mixing separated local field NMR spectroscopy. J Chem Phys. doi:10.1063/1.2212939

Fu R, Truong M, Saager RJ, Cotten M, Cross TA (2007) High-resolution heteronuclear correlation spectroscopy in solid state NMR of aligned samples. J Magn Reson 188:41–48. doi:10.1016/j.jmr.2007.06.004

Gopinath T, Veglia G (2009) Sensitivity enhancement in static solid-state NMR experiments via single- and multiple-quantum dipolar coherences. J Am Chem Soc 131:5754–5756. doi:10.1021/ja900096d

Gopinath T, Veglia G (2012a) 3D DUMAS: simultaneous acquisition of three-dimensional magic angle spinning solid-state NMR experiments of proteins. J Magn Reson 220:79–84. doi:10.1016/j.jmr.2012.04.006

Gopinath T, Veglia G (2012b) Dual acquisition magic-angle spinning solid-state NMR-spectroscopy: simultaneous acquisition of multidimensional spectra of biomacromolecules. Angew Chem 51:2731–2735. doi:10.1002/anie.201108132

Gopinath T, Veglia G (2013) Orphan spin operators enable the acquisition of multiple 2D and 3D magic angle spinning solid-state NMR spectra. J Chem Phys 138:184201. doi:10.1063/1.4803126

Gopinath T, Traaseth NJ, Mote K, Veglia G (2010a) Sensitivity enhanced heteronuclear correlation spectroscopy in multidimensional solid-state NMR of oriented systems via chemical shift coherences. J Am Chem Soc 132:5357–5363. doi:10.1021/ja905991s

Gopinath T, Verardi R, Traaseth NJ, Veglia G (2010b) Sensitivity enhancement of separated local field experiments: application to membrane proteins. J Phys Chem B 114:5089–5095. doi:10.1021/jp909778a

Gopinath T, Mote KR, Veglia G (2013) Sensitivity and resolution enhancement of oriented solid-state NMR: application to membrane proteins. Prog Nucl Magn Reson Spectrosc 75:50–68. doi:10.1016/j.pnmrs.2013.07.004

Gor'kov PL et al (2007) Using low-E resonators to reduce RF heating in biological samples for static solid-state NMR up to 900 MHz. J Magn Reson 185:77–93. doi:10.1016/j.jmr.2006.11.008

Hong M, Zhang Y, Hu F (2012) Membrane protein structure and dynamics from NMR spectroscopy. Annu Rev Phys Chem 63:1–24. doi:10.1146/annurev-physchem-032511-143731

Knox RW, Lu GJ, Opella SJ, Nevzorov AA (2010) A resonance assignment method for oriented-sample solid-state NMR of proteins. J Am Chem Soc 132:8255–8257. doi:10.1021/ja102932n

Manning G, Whyte DB, Martinez R, Hunter T, Sudarsanam S (2002) The protein kinase complement of the human genome. Science 298:1912–1934. doi:10.1126/science.1075762

Marassi FM, Opella SJ (2000) A solid-state NMR index of helical membrane protein structure and topology. J Magn Reson 144:150–155. doi:10.1006/jmre.2000.2035

Marassi FM, Ma C, Gesell JJ, Opella SJ (2000) Three-dimensional solid-state NMR spectroscopy is essential for resolution of resonances from in-plane residues in uniformly (15)N-labeled helical membrane proteins in oriented lipid bilayers. J Magn Reson 144:156–161. doi:10.1006/jmre.2000.2036

Mascioni A, Veglia G (2003) Theoretical analysis of residual dipolar coupling patterns in regular secondary structures of proteins. J Am Chem Soc 125:12520–12526. doi:10.1021/ja0354824

Mascioni A, Eggimann BL, Veglia G (2004) Determination of helical membrane protein topology using residual dipolar couplings and exhaustive search algorithm: application to phospholamban. Chem Phys Lipids 132:133–144. doi:10.1016/j.chemphyslip.2004.09.018

McDermott A (2009) Structure and dynamics of membrane proteins by magic angle spinning solid-state NMR. In: Annual review of biophysics, vol 38. pp 385–403. doi:10.1146/annurev.biophys.050708.133719

Mesleh MF, Veglia G, DeSilva TM, Marassi FM, Opella SJ (2002) Dipolar waves as NMR maps of protein structure. J Am Chem Soc 124:4206–4207

Miao Y, Cross TA (2013) Solid state NMR and protein-protein interactions in membranes. Curr Opin Struct Biol 23:919–928. doi:10.1016/j.sbi.2013.08.004

Michalek M, Salnikov ES, Bechinger B (2013) Structure and topology of the huntingtin 1–17 membrane anchor by a combined solution and solid-state NMR approach. Biophys J 105:699–710. doi:10.1016/j.bpj.2013.06.030

Mote KR, Gopinath T, Traaseth NJ, Kitchen J, Gor'kov PL, Brey WW, Veglia G (2011) Multidimensional oriented solid-state NMR experiments enable the sequential assignment of uniformly 15N labeled integral membrane proteins in magnetically aligned lipid bilayers. J Biomol NMR 51(3):339–346

Mote KR, Gopinath T, Veglia G (2013) Determination of structural topology of a membrane protein in lipid bilayers using polarization optimized experiments (POE) for static and MAS solid state NMR spectroscopy. J Biomol NMR 57:91–102. doi:10.1007/s10858-013-9766-2

Murray DT, Das N, Cross TA (2013) Solid state NMR strategy for characterizing native membrane protein structures. Acc Chem Res 46:2172–2181. doi:10.1021/ar3003442

Nevzorov AA (2008) Mismatched Hartmann–Hahn conditions cause proton-mediated intermolecular magnetization transfer between dilute low-spin nuclei in NMR of static solids. Journal of the American Chemical Society. doi:10.1021/ja804326b

Nevzorov AA, Park SH, Opella SJ (2007) Three-dimensional experiment for solid-state NMR of aligned protein samples in high field magnets. J Biomol Nmr 37:113–116. doi:10.1007/s10858-006-9121-y

Phillips R, Ursell T, Wiggins P, Sens P (2009) Emerging roles for lipids in shaping membrane-protein function. Nature 459:379–385. doi:10.1038/nature08147

Ramamoorthy A, Yamamoto K (2006) A family of PISEMA experiments for structural studies of biological solids. In: Webb G (ed) Modern magnetic resonance. Springer, Netherlands, pp 703–709

Resende JM, Verly RM, Aisenbrey C, Cesar A, Bertani P, Pilo-Veloso D, Bechinger B (2014) Membrane interactions of phylloseptin-1, -2, and -3 peptides by oriented solid-state NMR spectroscopy. Biophys J 107:901–911. doi:10.1016/j.bpj.2014.07.014

Shi L, Traaseth NJ, Verardi R, Cembran A, Gao J, Veglia G (2009) A refinement protocol to determine structure, topology, and depth of insertion of membrane proteins using hybrid solution and solid-state NMR restraints. J Biomol NMR 44:195–205. doi:10.1007/s10858-009-9328-9

Siegal G, van Duynhoven J, Baldus M (1999) Biomolecular NMR: recent advances in liquids, solids and screening. Curr Opin Chem Biol 3:530–536. doi:10.1016/s1367-5931(99)00004-6

Suter D, Enrnst RR (1985) Spin diffusion in resolved solid-state NMR spectra. Phys Rev B 32:5608–5627

Szeverenyi NM, Sullivan MJ, Maciel GE (1982) Observation of spin exchange by two-dimensional fourier transform 13C cross polarization-magic-angle spinning. J Magn Reson (1969) 47:462–475. doi:10.1016/0022-2364(82)90213-X

Tang W, Knox RW, Nevzorov AA (2012) A spectroscopic assignment technique for membrane proteins reconstituted in magnetically aligned bicelles. J Biomol NMR 54:307–316. doi:10.1007/s10858-012-9673-y

Traaseth NJ, Shi L, Verardi R, Mullen DG, Barany G, Veglia G (2009) Structure and topology of monomeric phospholamban in lipid membranes determined by a hybrid solution and solid-state NMR approach. Proc Natl Acad Sci USA 106:10165–10170. doi:10.1073/pnas.0904290106

Traaseth NJ, Gopinath T, Veglia G (2010) On the performance of spin diffusion NMR techniques in oriented solids: prospects for resonance assignments and distance measurements from separated local field experiments. J Phys Chem B 114:13872–13880. doi:10.1021/jp105718r

Veglia G, Traaseth NJ, Shi L, Verardi R, Gopinath T, Gustavsson M (2012) 1.11 The hybrid solution/solid-state nmr method for membrane protein structure determination. In: Egelman EH (ed) Comprehensive biophysics. Elsevier, Amsterdam, pp 182–198. doi:10.1016/B978-0-12-374920-8.00115-6

Verardi R, Shi L, Traaseth NJ, Walsh N, Veglia G (2011) Structural topology of phospholamban pentamer in lipid bilayers by a hybrid solution and solid-state NMR method. Proc Natl Acad Sci USA 108:9101–9106. doi:10.1073/pnas.1016535108

Vostrikov VV, Mote KR, Verardi R, Veglia G (2013) Structural dynamics and topology of phosphorylated phospholamban homopentamer reveal its role in the regulation of calcium transport. Structure. doi:10.1016/j.str.2013.09.008

Wang S, Ladizhansky V (2014) Recent advances in magic angle spinning solid state NMR of membrane proteins. Prog Nucl Magn Reson Spectrosc 82C:1–26. doi:10.1016/j.pnmrs.2014.07.001

Wang J, Denny J, Tian C, Kim S, Mo Y, Kovacs F, Song Z, Nishimura K, Gan Z, Fu R, Quine JR, Cross TA (2000) Imaging membrane protein helical wheels. J Magn Reson 144:162–167. doi:10.1006/jmre.2000.2037

Waugh JS (1976) Uncoupling of local field spectra in nuclear magnetic-resonance—determination of atomic positions in solids. Proc Natl Acad Sci USA 73:1394–1397. doi:10.1073/pnas.73.5.1394

Wu CH, Ramamoorthy A, Opella SJ (1994) High-resolution heteronuclear dipolar solid-state NMR-spectroscopy. J Magn Reson Ser A 109:270–272. doi:10.1006/jmra.1994.1169

Wu CH, Ramamoorthy A, Gierasch LM, Opella SJ (1995) Simultaneous characterization of the amide H1 chemical shift, H1–N15 dipolar, and N15 chemical-shift interaction tensors in a peptide-bond by 3-dimensional solid-state NMR Spectroscopy. J Am Chem Soc 117:6148–6149. doi:10.1021/ja00127a039

Xu J, Struppe J, Ramamoorthy A (2008) Two-dimensional homonuclear chemical shift correlation established by the cross-relaxation driven spin diffusion in solids. J Chem Phys. doi:10.1063/1.2826323